

TUTORIAL OPEN ACCESS

Disease Progression Mathematical Modeling With a Case Study on Hepatitis B Virus Infection

Clémence Boivin-Champeaux¹  | Nieves Velez de Mendizabal² | Aksana Jones²  | Scott Balsitis³  |
Stephan Schmidt¹  | Justin S. Feigelman²  | Francine Johansson Azeredo¹ 

¹Department of Pharmaceutics, Center for Pharmacometrics and Systems Pharmacology, College of Pharmacy, University of Florida, Orlando, Florida, USA | ²Clinical Pharmacology and Pharmacometrics, Gilead Sciences, Foster City, California, USA | ³Research Discovery Virology, Gilead Sciences, Foster City, California, USA

Correspondence: Justin S. Feigelman (justin.feigelman@gilead.com) | Francine Johansson Azeredo (francinej@ufl.edu)

Received: 31 May 2024 | **Revised:** 10 December 2024 | **Accepted:** 12 December 2024

Funding: The authors received no specific funding for this work.

Keywords: disease progression | HBV | mathematical modeling | viral dynamics

ABSTRACT

Chronic Hepatitis B presents a significant health and socioeconomic burden. The risk of hepatocellular carcinoma remains elevated although treatments are available. Achieving an optimal treatment regimen necessitates a deep comprehension of the dynamic relationship between the virus and its host across disease states. This tutorial elucidates essential considerations for establishing a disease modeling platform to facilitate informed decision-making in hepatitis B treatment strategies. We review several published models of varying complexity and describe the context that motivated each model's structure and assumptions. Several of the models are made available in an interactive RShiny app to demonstrate the influence of model choice and sensitivity to the choice of parameter values.

1 | Introduction

Chronic hepatitis B (CHB) represents a significant global health challenge, leading to severe complications, such as cirrhosis and hepatocellular carcinoma, caused by Hepatitis B virus (HBV), a noncytotoxic, hepatotropic, double-stranded DNA virus. According to the World Health Organization's 2024 report, approximately 254 million individuals were living with CHB in 2022, resulting in an estimated 1.1 million deaths. Additionally, 1.2 million new HBV infections were estimated to have occurred in the same year. The economic burden is significant, with projections from The Lancet Gastroenterology and Hepatology estimating that hepatitis B-related deaths could lead to over \$780 billion in economic loss between 2022 and 2050 without increased investment in prevention and treatment interventions.

There is currently no cure for CHB despite advances in hepatitis B treatment. This is, at least in part, due to the complex

pathobiology of the disease, which resembles a dynamic interplay between the virus and the host's immune system. Understanding this interplay is non-trivial but can be aided through the use of mechanistic models, which can be used to simulate the impact of novel and existing treatments on viral replication, immune response, and disease progression. This may facilitate the identification of drug targets, optimization of treatment and dosing regimens, and design of more effective clinical trials, ultimately improving patient outcomes. Establishing such mechanistic models requires a deep understanding of the underlying pathobiology and associated dynamic behavior of the biological system.

This tutorial offers a step-by-step guide to developing a mechanistic HBV model by first reviewing the key biological aspects of HBV infections, including viral entry, replication, immunopathology, and biomarkers relevant to both acute and chronic phases of the disease before translating these aspects into

This is an open access article under the terms of the [Creative Commons Attribution-NonCommercial-NoDerivs](https://creativecommons.org/licenses/by-nc-nd/4.0/) License, which permits use and distribution in any medium, provided the original work is properly cited, the use is non-commercial and no modifications or adaptations are made.

© 2024 The Author(s). *CPT: Pharmacometrics & Systems Pharmacology* published by Wiley Periodicals LLC on behalf of American Society for Clinical Pharmacology and Therapeutics.

mechanistic models of increasing complexity that encompass the distinct HBV infection phases. Throughout this iterative process, we will highlight key biological aspects driving model complexity, strengths and limitations of the different models as well as the critical role of data in model development, refinement, and validation.

2 | Hepatitis Virus Infection Pathophysiology

It is first necessary to thoroughly understand the mechanisms and pathways underlying the disease to develop a detailed, mechanistic model of HBV infection. In the following sections, we provide a summary of the current understanding of HBV infection, control by the host immune system, and the various biomarkers that define each phase of the disease. This detailed understanding will serve as the scientific basis for later modeling and application to therapeutic research and development.

2.1 | HBV Viral Entry

HBV infects hepatocytes and replicates in a complex, multistep process involving several viral proteins as well as various forms of DNA and RNAs, summarized in Figure 1. The virulent form of HBV, also known as a Dane particle, comprises partially double-stranded, relaxed circular deoxyribonucleic acid (rcDNA) bound to a polymerase, enclosed within a nucleocapsid and a lipid membrane envelope containing three variations of the HBV surface antigen (HBsAg): small (S), middle (M), and large (L) proteins. Once transmitted, the envelope proteins bind primarily to hepatocytes [1–3], delivering the virion's genome into the cell. Hepatocellular binding of HBV occurs predominantly on the surface of hepatocytes spanning from the space of Disse to the lumen of the sinusoids [1–3], mediated by selective, low-affinity binding to heparin sulfate proteoglycans (HSPGs). HBV's liver tropism is also largely attributed to its strong binding affinity to the sodium taurocholate co-transporting polypeptide (NTCP) receptor, which is abundantly expressed on the basolateral

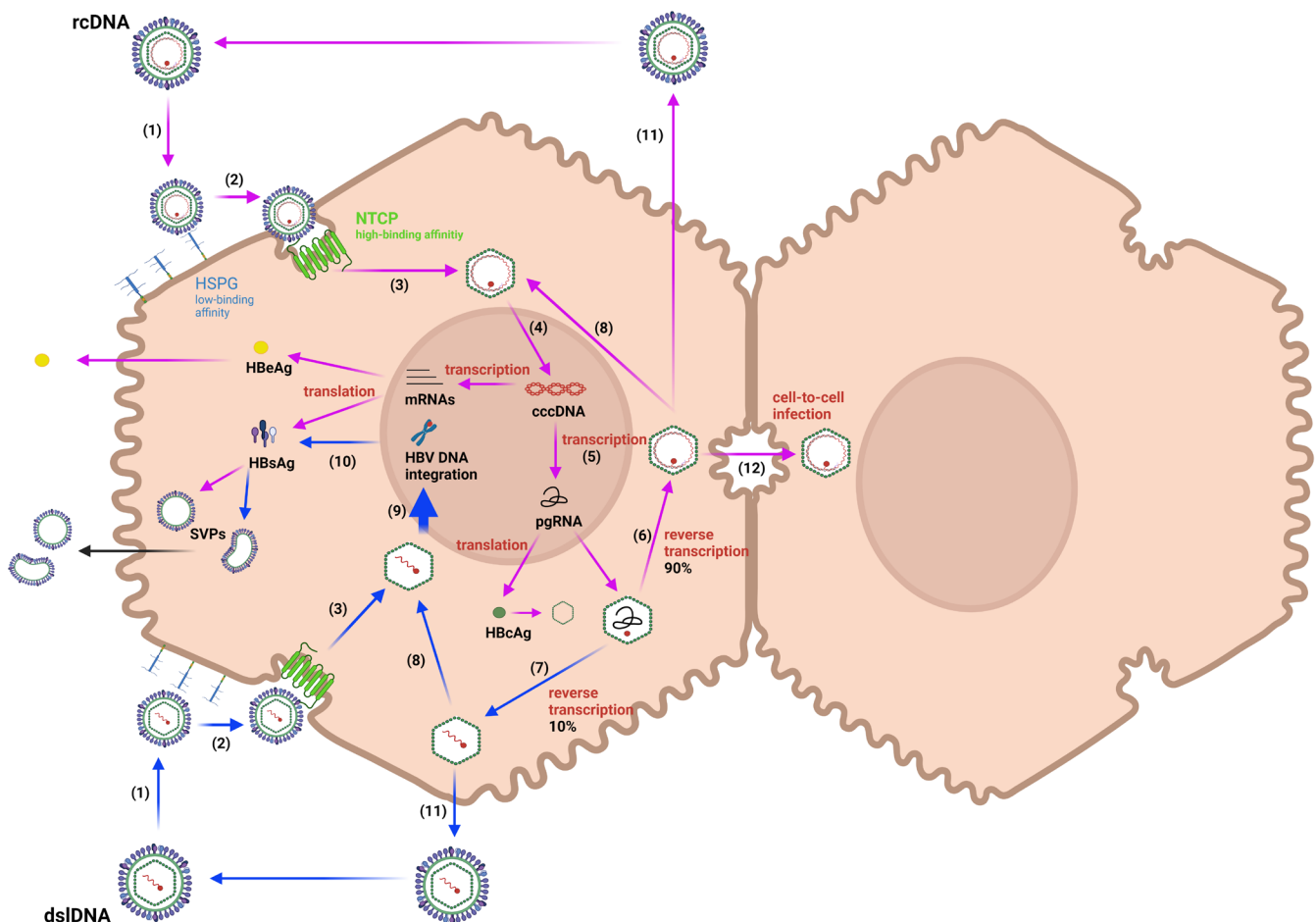


FIGURE 1 | HBV life cycle: Depiction of the lifecycle of HBV from its entry into a host hepatocyte to the production of infectious and non-infectious particles. Upon transmission, HBV enters hepatocytes primarily through binding hepatocyte surface receptors such as (1) HSPG and then (2) NTCP with subsequent endocytosis. The viral genome is then released (3) into the cytoplasm and (4) transported to the nucleus, where it forms cccDNA. Replication of HBV involves (5) transcription of pgRNA from cccDNA, encapsidation of pgRNA with viral polymerase and core protein, and reverse transcription to generate new (6) rcDNA or (7) dsIDNA. These newly synthesized genomes can either (8) replenish the cccDNA pool or (9) dsIDNA can integrate into the host genome. (10) Translation of viral mRNAs leads to the production of HBsAg and HBeAg. (11) Mature virions bud into the bloodstream from infected hepatocytes. (12) HBV transmission may also occur paracellularly through the bile canalculus channel between adjacent hepatocytes. The purple and blue arrows represent the rcDNA-related processes and the dsIDNA-related processes, respectively. The black arrow represents both rcDNA- and dsIDNA-related processes (production of SVP particles).

membrane of human hepatocytes [1–3]. Following binding, the virus is thought to penetrate the cell through clathrin-mediated endocytosis. After endocytosis, HBV traffics through the early and late endosomal compartments and undergoes cytosolic release, resulting in the removal of the viral envelope [1]. The free nucleocapsid then translocated to the nucleus through the microtubule network. Upon reaching the nuclear pore complex, the nucleocapsid disassembles and discharges the rcDNA genome along with its covalently attached polymerase into the nucleoplasm, initiating the replication phase of the virus [2].

2.2 | HBV Replication

Several host factors are crucial in modifying and repairing the nuclear rcDNA during replication [2, 4, 5], ultimately forming the covalently closed circular DNA (cccDNA) that encodes viral proteins [4, 5]. Pre-genomic RNA (pgRNA) transcribed from the cccDNA encodes both HBV Pol and HBV core protein (HBcAg) [3]. HBcAg protein self-assembles to form the inner nucleocapsid enclosing the viral DNA, typically comprising 240 HBcAg copies [6]. Subsequently, pgRNA is encapsidated with Pol and reverse transcribed, producing a nucleocapsid containing either rcDNA (90%) or double-stranded linear DNA (dsLDNA, 10%) [7]. The newly formed rcDNA and dsLDNA can either traffic back to the nucleus, amplifying the pool of cccDNA, or integrate into the host genome in case of recirculated dsLDNAs [3, 7]. Subsequent transcription of both the integrated viral genome and cccDNA yield viral mRNAs. These mRNAs code for HBV surface antigen proteins (HBsAg), which in complex with nucleocapsids, bud into the lumen of multivesicular bodies (MVBs) [3, 7] and release into the bloodstream as mature virions containing HBV DNA [2, 3, 8]. Therefore, circulating HBV DNA is found only in mature virions produced exclusively by hepatocytes containing cccDNA. Similarly, cccDNA-produced mRNAs also produce the pre-core protein p22cr which is processed into hepatitis B e antigen (HBeAg), which is secreted and circulates in serum [3]. HBsAg also contributes to abundant formation of noninfectious subviral particles (SVPs) in the bloodstream, outnumbering virions by a factor of up to 100,000 [2, 3, 9]. Notably, dsLDNA integration cannot support viral replication. Instead, it typically leads to the expression of the three forms of HBsAg [3, 7] and potentially fragments of the HBV-encoded oncogene X protein (HBx). HBx, a key multifunctional regulatory protein, not only drives viral replication but also interferes with several cellular signaling pathways, contributing to virus-associated hepatocarcinogenesis [10]. Following the initial viral replication, the host immune system may initiate a response.

2.3 | HBV Immunopathology

Most healthy adults newly infected with HBV typically experience short-lived, asymptomatic infections lasting under 6 months, known as acute hepatitis B (AHB) [11, 12], which reflects effective viral control by the host immune system. However, some infections progress to CHB, most commonly in infants and young children [11, 12]: 90%–95% of CHB cases arise from perinatal HBV infection compared to <5% in immunocompetent adults [3, 11, 13].

2.3.1 | Acute Hepatitis B

Host immune responses usually clear the virus from the body during AHB [3]. Following an initial innate immune response, cellular immune responses including both CD4 and CD8+ T cells are then activated and play a crucial role in clearing the virus through both cytolytic (i.e., eliminating infected hepatocytes) [3], and potentially non-cytolytic mechanisms involving IFN- γ and TNF- α [14]. The humoral immune response also frequently aids in clearing circulating viral and subviral particles, thereby hindering viral dissemination, though its precise control in viral control remains uncertain [3, 15].

2.3.2 | Chronic Hepatitis B

Adaptive immune responses to HBV are weak to undetectable in CHB patients in contrast to cases of acute clearance [3, 16]. This results in sustained viral persistence and many CHB patients remain asymptomatic for decades before diagnosis. CHB progresses through distinct phases (see Figure 2C), each marked by unique clinical presentations that arise from specific underlying biological processes [11, 13, 16–18]. Importantly, these phases are dynamic and not strictly sequential; patients may transition between phases in any direction [17].

2.3.2.1 | HBeAg-Positive Infection Phase. The initial phase of CHB, known as the HBeAg-positive infection phase, is characterized by a limited host immune response toward infected hepatocytes, resulting in an asymptomatic presentation [13, 17, 18]. While the precise mechanisms underlying this immunotolerance remain incompletely understood and still subject of ongoing investigation and controversy, multiple factors are thought to contribute to it. HBV antigen presentation by hepatocytes in the absence of effective co-stimulation may produce a tolerance-like phenotype in T cells distinct from classical exhaustion [19]. HBeAg is hypothesized to act as an immune tolerogen, desensitizing the T-cell response [20]. SVPs are believed to contribute as well by producing high levels of HBsAg, which may overwhelm anti-HBsAg antibody responses. Additionally, an imbalance of regulatory T cells (Tregs) [21, 22] and Th17 cells may impair CD8+ T-cell proliferation, further dampening the immune response [23].

2.3.2.2 | HBeAg-Positive Hepatitis Phase. As the host's immune system becomes more effective in clearing HBV, a second phase, known as the HBeAg-positive hepatitis phase, may emerge. This phase is characterized by the partial immune-mediated elimination of infected hepatocytes, resulting in chronic liver inflammation and a degree of immune control over viral replication [13, 17, 18]. The loss of HBeAg in this phase often signifies a favorable prognosis, especially when it occurs at a young age [24].

2.3.2.3 | HBeAg-Negative Infection and HBeAg-Negative Hepatitis Phases. Following the loss of circulating HBeAg, patients may progress to either HBeAg-negative infection phase, in which alanine transaminase (ALT), a biomarker for liver injury, is not elevated, or the HBeAg-negative hepatitis

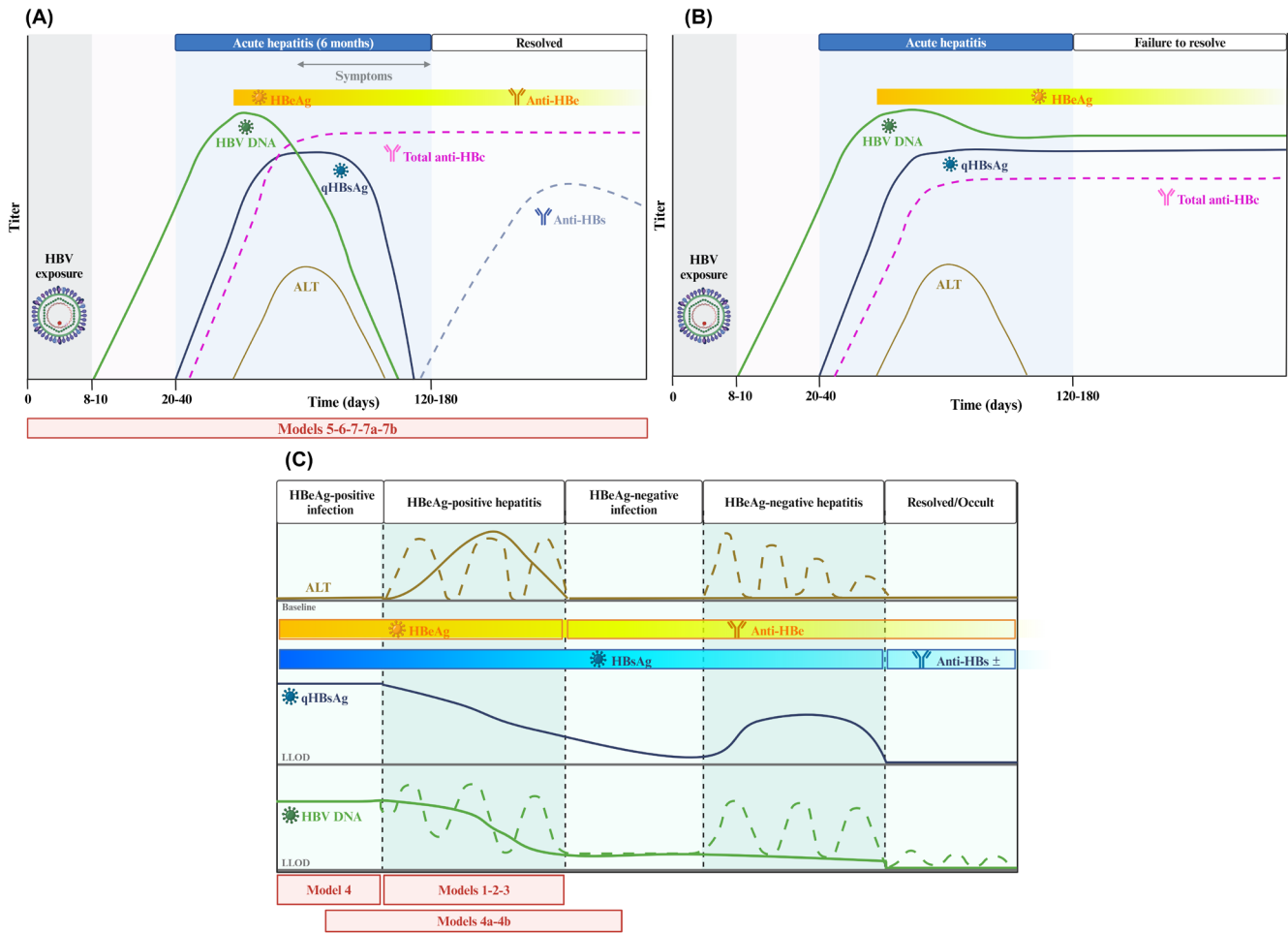


FIGURE 2 | (A) Time course of acute hepatitis B infection with recovery: Short-lived HBV infection since the patient successfully controls the virus. After exposure, there is an eclipse phase lasting approximately 8 days, followed by a window period where HBV DNA (solid green line) can be detected, but HBsAg (solid blue line) is still absent. Around 35 days post-exposure, HBsAg becomes detectable, followed by the appearance of anti-HBc antibodies (pink dashed line). As the infection resolves, HBsAg levels decrease, and anti-HBc levels rise. A second window phase may occur after HBsAg disappears but before anti-HBs (blue dashed line) are detectable, depending on the assay used. During this period, anti-HBc is the only marker of infection. Over time, anti-HBs levels may drop and become undetectable, leaving anti-HBc as the sole indicator of past HBV exposure. The disappearance of HBsAg and concomitant increase in anti-HBsAg signifies the resolution of AHB. (B) Time course of acute hepatitis B infection without recovery: The infection is starting to transition from an acute state to a chronic condition despite the involvement of the adaptive immune response to contain and clear the viral infection. HBV DNA (solid green line) and HBsAg (solid blue line) are not cleared and there is no anti-HBs. (C) Time course of chronic hepatitis B infection: Chronic infections categorized into distinct phases, each characterized by a unique clinical phenotype as the result of distinct underlying biological processes. The dashed lines for HBV DNA (green dashed line) and ALT (brown dashed line) represent intermittent flares indicating increased liver inflammation or damage. These flares can be triggered by immune responses or changes in viral replication. The frequency of these episodes can vary among individuals. HBV, Hepatitis B virus; DNA, deoxyribonucleic acid; qHBsAg, quantitative hepatitis B surface antigen; HBeAg, hepatitis B e antigen; anti-HBs, antibodies to surface antigen; anti-HBe, antibodies to e antigen; ALT, alanine transaminase; LLOD, lower limit of detection. Adapted from [17].

phase, in which chronically elevated ALT persists. Individuals may enter these phases in either order and may revert between them [25].

2.3.2.4 | Resolved/Occult Phases. In some individuals, robust CD8 T-cell responses successfully clear nearly all HBV+ cells, achieving a “functional cure” defined as persistently undetectable HBsAg and HBV DNA in plasma. Others in rare cases may enter the occult phase, defined as detectable HBV DNA despite HBsAg negativity indicating a persistent low-level infection driven by the immune system’s inability to eliminate latent reservoirs. Occult infection can be misdiagnosed as resolved

infection [13, 17, 26], if HBsAg levels are tested without simultaneous measurement of HBV DNA.

2.4 | Biomarkers

Biomarkers provide critical insights into the origins, biological responses, and clinical presentation of a disease. One critical parameter is HBV transcriptional activity in HBV+ hepatocytes. Since direct measurement of cccDNA or integrated HBV is challenging due to the invasive nature of liver biopsies [17, 18, 26], secondary biomarkers of HBV infection are frequently employed

to characterize infection dynamics. Critically, biomarker data generated through clinical trials facilitates the development of mathematical models describing these dynamics.

2.4.1 | Biomarkers for Acute Hepatitis B

AHB infection results in a set of biomarker trajectories (Figure 2A). HBV DNA and HBsAg levels sharply increase as the virus rapidly replicates in the liver post-infection. Subsequently, elevated liver enzymes (ALT) appear in serum as immune-mediated cytolysis of HBV+ cells begins, and clinical hepatitis signs may appear. Serum HBeAg is often detected immediately after HBsAg is first detected. As the immune response starts to control the infection, HBV DNA levels gradually decline, followed by HBsAg levels. HBeAg becomes undetectable as anti-HBe antibodies arise. The disappearance of HBsAg and the simultaneous emergence of anti-HB antibodies often signifies AHB resolution [17, 18, 26]. In contrast, if viremia fails to be suppressed, HBsAg and HBV DNA continue to remain elevated (Figure 2B).

2.4.2 | Biomarkers for Chronic Hepatitis B

CHB may progress through a number of phases with distinct biomarker profiles as shown in Figure 2C. Each phase is marked by distinct profiles for HBV DNA, HBsAg, HBeAg, and ALT. The HBeAg-positive infection phase is marked by high levels of HBV DNA and HBsAg, the presence of HBeAg with a low rate of spontaneous clearance [27], and normal or slightly elevated serum ALT levels. In contrast, the HBeAg-positive hepatitis phase is characterized by gradual decreases in HBV DNA and HBsAg levels, coupled with increased ALT, decreased HBeAg, and a potential seroconversion to HBeAg-negative and anti-HBeAg antibody positive [13, 17, 18, 26–28]. In the HBeAg-negative infection phase, HBeAg is not detected, HBV DNA levels are reduced, and ALT levels are in the normal range. However, HBsAg expression persists due to integrated DNA and residual cccDNA [13, 17, 18, 26–28]. If ALT becomes elevated, the infection stage is characterized as HBeAg-negative hepatitis. HBV DNA and HBsAg may show transient or persistent elevation during this phase. HBeAg seroreversion may also occur, emphasizing the need for continued monitoring [13, 17, 18, 26–28]. Lastly, both the resolved and occult phases are characterized by the loss of HBsAg, with anti-HBs potentially present or absent in either phase [13, 17, 18, 26–28]. Notably, many individuals spontaneously clear HBsAg without developing detectable anti-HB antibodies [29]. In the resolved phase, HBV DNA becomes undetectable, whereas in occult HBV, viral DNA remains detectable, typically in the liver and occasionally in serum. Additional biomarkers, including serum HBV RNAs and hepatitis B core-related antigen (HBcrAg), may also be clinically meaningful [17].

3 | Disease Progression Modeling

Disease progression models aim to comprehend the natural evolution of the disease, mimicking its clinical features and biomarkers in either treated or untreated conditions. Significant effort is required to ensure that the model structure aligns appropriately with the specific research objectives/context of use,

with the intricacy of the question at hand determining the appropriate level of model complexity. In particular, more complex semi-mechanistic and quantitative systems pharmacology models may be more suitable for predicting drug effects, identifying therapeutic targets, optimizing dose selection, refining trial designs, making go/no-go decisions in drug development, and assessing risks based on available biomarker data [30].

Semi-mechanistic models of varying levels of complexity have been developed over the years in HBV. Many models have been previously developed for a variety of viruses with different tissue tropisms, including HIV or hepatitis C virus. However, HBV exhibits unique clinical features such as lack of cell lysis following infection, which ultimately led to the development of models considering its unique biology with increasing levels of complexity. These models exist in the context of a large space of viral and/or immune cell dynamics that continue to evolve, driven by ongoing biological discoveries. In the following sections, we illustrate the intricate process involved in constructing such models, with each model driven by specific research goals and available data. These models contain various elements of HBV infectious biology as described in the previous sections. For an overview of the key biological processes captured by each model, refer to Table S1. Parameter values and initial conditions for Models 1–7b are provided (Tables S2 and S3 respectively), enabling readers to utilize this tutorial as a practical resource for constructing their own models of HBV infection and disease progression. Additionally, a set of models of acute HBV infection were implemented in Shiny within Rstudio and are made available in the Supporting Information (Github link or Code S1 and S2). Two apps are available that implement Models 5, 6, 7a, and 7b and provide the capability to adjust parameter values and initial conditions in the mean profiles within the app to observe their influence on viral dynamics, and the capability to observe the models' fit to the individual profiles.

3.1 | Chronic HBV Models

3.1.1 | Basic Virus Infection Model (BVIM)

Nowak et al. [31] developed one of the first semi-mechanistic modeling frameworks for HBV infection building upon approaches used to investigate the dynamics of viral infections like human immunodeficiency virus (HIV) and hepatitis C virus (HCV). Subsequent studies, such as those conducted by Tsiang et al. [32] and Lau et al. [33], adopted similar model structures as Nowak et al. to describe HBV viral dynamics with a focus on three distinct entities: target uninfected hepatocytes (T), infected hepatocytes (I), and free virus (V). We refer to this system as Model 1, shown in Figure 3.

In this model, healthy hepatocytes are produced at a constant rate, such as from a source of progenitor cells outside the liver. Uninfected hepatocytes can then be infected in the presence of HBV. Because HBV is considered a non-cytopathic virus, the elimination of infected cells encompasses the innate response and the cytolytic processes induced by the host's immune system. The mechanism of virion clearance is not specified but may occur through the reticuloendothelial function of the liver, by the formation of antibody–virus complexes and subsequent

[Model 1].

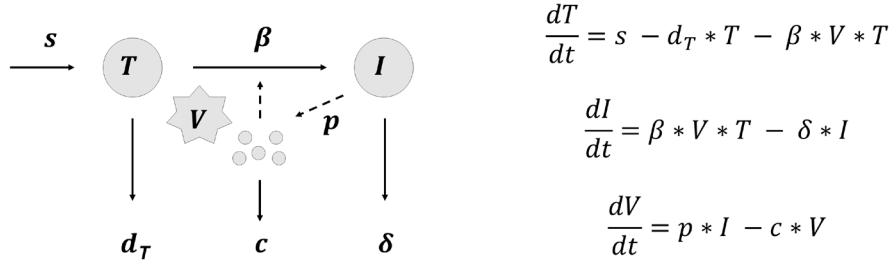


FIGURE 3 | [Model 1]. Basic virus infection model (BVIM), chronic HBV. Three compartments: T , target uninfected hepatocytes; I , infected hepatocytes; V , hepatitis B virus. s , production constant rate of target cells; d_T , uninfected cells death rate; β , infection rate; δ , infected cells death rate; p , virions production rate from infected cells; c , virions clearance rate.

phagocytosis, or other mechanisms. The aforementioned authors used Model 1 to fit the kinetics of viral decay, using plasma HBV viral load data from chronic HBeAg-positive patients under different treatments, and estimated the kinetic constants governing viral infection, cell death, and the efficacy of antiviral therapy.

The models used in each of these publications differ somewhat in their assumptions although structurally the same. Initially, Tsiang et al. [32] aligned their assumptions with those of Nowak et al. [31] in their data analysis. However, the viral load function failed to adequately fit the observed data throughout the study duration. This led to them rejecting the assumption that the number of infected cells remains constant during therapy. While this approximation is valid for a brief period after therapy initiation, it loses accuracy when applied to an extended therapy period. This updated assumption is biologically plausible and, based on their results, provides a more accurate fit to the data. Delving deeper into the mathematical representation, Model 1 reveals certain limitations. The viral infection process is assumed to follow mass action kinetics proportional to free virions and healthy cells, with rate constant β . While this approach captures the overall infection rate, it fails to explicitly account for the underlying infection mechanism. This assumption suggests that the rate of contact between healthy target cells and free virions is the primary factor influencing infection, overlooking potential saturation effects or variations in infectiousness. Consequently, β lacks a clear biological interpretation [34, 35]. Another issue arises when considering the basic infection reproductive number, R_0 , defined by $\frac{s * \beta * p}{\delta * d_T * c}$. This metric estimates the number of secondary infections per infected cell at the onset of infection if susceptible cells are not depleted. If R_0 exceeds 1, the infection spreads; if it is below 1, the infection subsides.

If the quantity T represents the absolute number of cells rather than a concentration, then the steady-state number of cells before infection is given by $\frac{s}{d_T}$. However, this would imply that individuals with smaller livers (and thus fewer liver cells), such as children, might exhibit greater resistance to viral infections than adults with larger livers, which is biologically implausible [34, 35]. This relationship between R_0 and $\frac{s}{d_T}$ appears to be also an artifact of the mass action formulation, often unsuitable for infection dynamics involving numerous hosts, such as cells, especially when the total cell count varies [35]. However, this

phenomenon does not occur when treating T and I as concentrations, as is more frequently the case for this model.

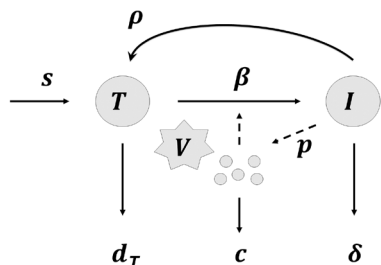
For these early models, variations in the treatments and quantification methods for serum HBV DNA, as well as different model assumptions led to different estimates of parameter values between Lau et al.'s study [33] and the other two [31, 32], rendering it difficult to draw definitive model-based conclusions regarding CHB infection [36, 37]. The reader can refer to Table S2 which includes the parameter estimates for the different studies cited for model version 1.

3.1.2 | Non-Cytolytic Process

A later study by Lewin et al. [38] analyzed serum HBV DNA data from HBeAg-positive chronic hepatitis B patients undergoing antiviral treatment. The authors observed that some patients exhibited a complex pattern characterized by phases of viral decline interspersed with periods of minimal change in viral load, a pattern not captured by earlier models. These intricate decay profiles pointed to an additional mechanism of infected cell loss beyond the cytolytic pathway, highlighting the complex interplay between the virus, cells, and the host immune response in CHB. Lewin et al. proposed an updated model (Model 2, shown in Figure 4) that incorporates a non-cytolytic pathway for infected cell clearance to address this. This mechanism, involving the clearance of cccDNA from infected cells and their reversion to an uninfected state, was backed by observations made by Guidotti et al. showing that CD8+ T cells clear HBV cccDNA from the nucleus and HBV replicative intermediates from hepatocyte cytoplasm without inducing cytotoxicity via the action of inflammatory cytokines such as IFN- γ and TNF- α [39].

New experimental data generated through molecular beacons and real-time PCR, accurately quantified HBV viral titers across a wide range, revealing heterogeneity in viral decay profiles that previous models did not capture. The observed decay patterns, such as plateau phases and staircase declines, indicate that prior models' biphasic assumptions were insufficient to capture these dynamics. By incorporating non-cytolytic mechanisms and potential delays before drug efficacy, this updated model aligns more closely with observed HBV DNA data, accommodating the individual variability seen in HBV patients under treatment, thereby improving predictive accuracy compared to simpler

[Model 2].



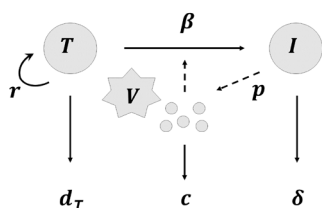
$$\frac{dT}{dt} = s - d_T * T - \beta * V * T + \rho * I$$

$$\frac{dI}{dt} = \beta * V * T - \delta * I - \rho * I$$

$$\frac{dV}{dt} = p * I - c * V$$

FIGURE 4 | [Model 2]. Chronic HBV. Three compartments: T , target uninfected hepatocytes; I , infected hepatocytes; V , hepatitis B virus; s , production constant rate of target cells; d_T , uninfected cells death rate; β , infection rate; δ , infected cells death rate; p , virions production rate from infected cells; c , virions clearance rate; ρ , noncytolytic cure rate of infected cells.

[Model 3].



$$\frac{dT}{dt} = r * T * \left(1 - \frac{T + I}{T_{max}}\right) - d_T * T - \beta * V * \frac{T}{T + I}$$

$$\frac{dI}{dt} = \beta * V * \frac{T}{T + I} - \delta * I$$

$$\frac{dV}{dt} = p * I - c * V$$

FIGURE 5 | [Model 3]. Chronic HBV. Three compartments: T , target uninfected hepatocytes; I , infected hepatocytes; V , hepatitis B virus; s , production constant rate of target cells; d_T , uninfected cells death rate; β , infection rate; δ , infected cells death rate; p , virions production rate from infected cells; c , virions clearance rate; ρ , noncytolytic cure rate of infected cells; T_{max} , maximum carrying capacity; r , maximum proliferation rate.

models used in earlier research. The final model parameters are shown in Table S2.

3.1.3 | Uninfected Hepatocyte Proliferation and Standard Incidence Function

To overcome the previously mentioned issues arising from the mass action treatment of viral uptake, later models by Min et al. [34], Gourley et al. [35], Eikenberry et al. [40], and Hews et al. [41] introduced a “standard incidence function,” which incorporates a maximum infection rate, β , defining the rate at which healthy cells become infected. By dividing the product of healthy cells and free virions by the total population size ($T + I$), it normalizes the infection rate, reflecting the proportion of healthy cells available for infection. While both formulations describe the infection rate within a population, the standard incidence function provides a clearer biological interpretation of β , as the maximum infection rate of the virus. It accounts for population size and explicitly links β to the probability of infection per contact, making it more biologically meaningful within the context of infectious disease infection.

Another simplifying assumption made in the previous models is that uninfected hepatocytes are produced at a constant rate. However, this approach does not consider constraints to hepatocyte proliferation, such as regulatory feedback mechanisms or limited nutrient supply [42]. Thus, some models replaced this term with a logistic growth function dependent on the current number of hepatocytes and a hypothetical maximum capacity for hepatocytes [40, 41]. The updated model is more biologically

plausible as it considers regulated liver regeneration dependent on the actual mass of the liver. We refer to this updated model with these two changes, as Model 3, shown in Figure 5.

Min et al. [34] applied their model to clinical HBV infection data (specifically, HBeAg-positive chronic hepatitis B patients from Lau et al. [33]). The simulation results closely matched the reported clinical data, demonstrating better agreement with clinical trials compared to Model 1. Eikenberry et al. [40] and Hews et al. [41] emphasized that incorporating logistic proliferation enriches the dynamics, introducing the possibility of sustained oscillations alongside the well-known asymptotic behaviors. This periodic behavior mirrors repeated cycles of acute liver damage, viral clearance, and spontaneous recovery seen clinically as acute liver failure (ALF) [40]. ALF can manifest suddenly, characterized by widespread hepatocyte necrosis and massive immune activation, potentially leading to death [43].

While the updated model is more realistic, it still lacks the representation for numerous aspects of pathophysiology such as varying cccDNA copies, different types of HBV particles, cell-to-cell transmission, or proliferation of infected hepatocytes and its influence on viral replication in the context of chronic disease. Subsequent models aim to address these limitations through additional model complexity.

3.1.4 | HBeAg and Immune Tolerance

One aspect not yet explored in previous HBV infection models is the influence of different viral proteins found in serum upon

viral dynamics. Ciupe et al. [44] investigated the role of viral antigens in immunotolerance, particularly focusing on serum HBeAg, which is believed to play a role in inducing immunotolerance by inactivating HBeAg-specific CD8+ T cells, for example, via clonal deletion, ignorance, or anergy (inability of HBeAg-specific T cells to grow, mature, and acquire effector function such as cytokine production) [44, 45]. To establish a connection between processes leading to HBeAg clearance, emergence of potent cellular immune response, and liver damage, they developed a model we refer to as Model 4 (Figure 6). This model comprises HBeAg+ virus, HBeAg, and HBeAg-specific T cells. They simplified the viral life cycle into a straightforward replication model by incorporating hepatocyte infection and viral production dynamics into a single virus equation. Upon encountering the antigen, antigen-specific T cells undergo activation, expansion, and differentiation into cytotoxic killer cells. The model limits T-cell expansion to represent immunological tolerance. Virus elimination is mediated by “immune cells,” assuming a quasi-equilibrium between the virus and infected liver cells, as immune cells are not represented as directly eliminating the virus.

In the immune clearance phase of CHB, HBeAg is lost. This loss is presumed to be due to either spontaneous HBeAg seroconversion or mutations leading to loss of viral antigen. To capture this, the authors introduced a model considering

either HBeAg seroconversion (Model 4a) or HBeAg- mutation (Model 4b). Model 4a assumes constant HBeAb concentration at its maximal size, and Model 4b assumes a constant percentage ϕ of strain V_{e+} mutating to give rise to virus V_{e-} , and no cross-reactivity between T-cell responses to HBeAg-negative and HBeAg-positive viruses [46].

When the seroconversion is instantaneous or the mutation rate is high, both scenarios are linked to minimal liver damage and better disease prognosis. The model also suggests that HBeAg induces T-cell tolerance by reducing proliferative capabilities but not killing abilities. However, it simplifies the actual biology by solely attributing T-cell inhibition to HBeAg, ignoring contributions from factors like HBeAg and Tregs, or the imbalance between Tregs and Th17. The age of tolerance loss is also overlooked, which may impact infection severity. Despite these simplifications, the study predicts dynamics during tolerance loss, aiding in understanding its desirability and potential negative long-term liver effects.

The model by Kadelka et al. [45] further explores the roles of HBeAg. It predicts the interplay between cellular and antibody responses on HBeAg seroclearance, incorporating uninfected and infected hepatocytes, virus, HBeAg, effector cells, HBeAb, and HBeAg-HBeAb immune complexes. This model is further modified to include core and precore mutations.

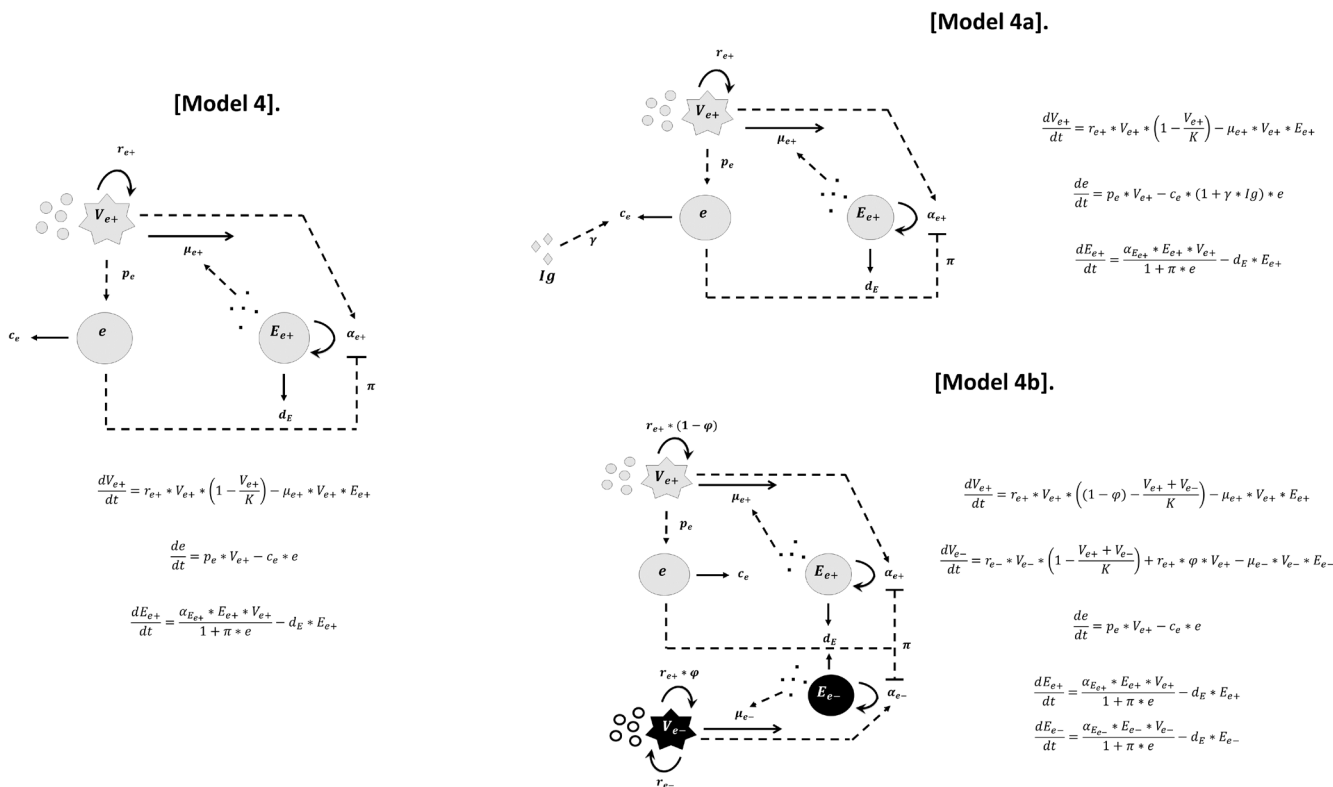


FIGURE 6 | [Model 4]. Chronic HBV (Immune tolerant phase). Three compartments: V_{e+} , HBeAg-positive virus; e , HBeAg; E_{e+} , HBeAg-specific T cells. r_{e+} , HBV production rate; K , maximum carrying capacity; μ_{e+} , immune-mediated killing; p_e , production rate of HBeAg; c_e , clearance rate of HBeAg; $\alpha_{E_{e+}}$, E_{e+} activation rate; $\pi * e$, immunological tolerance governed by limiting T-cell expansion to a maximum quantity with π being the strength of e -antigen inhibition. [Model 4a]. Chronic HBV (Loss of Immune tolerant phase, Seroconversion). Three compartments: V_{e+} , HBeAg-positive virus; e , HBeAg; E_{e+} , HBeAg-specific T cells. γ , antibody-mediated HBeAg removal rate; I_g , HBeAb. [Model 4b]. Chronic HBV (loss of immune tolerant phase, mutations in the core promoter or precore region). Five compartments: V_{e+} , HBeAg-positive virus; e , HBeAg; E_{e+} , HBeAg-specific T cells; V_{e-} , HBeAg-negative virus strains; E_{e-} , V_{e-} specific T-cell. ϕ , mutation percentage.

3.1.5 | Occult HBV Model

The occult phase of HBV infection remains poorly understood due to limited biomarker data availability. Goyal et al. [47] tackled this challenge by employing mathematical modeling to elucidate the dynamics of the transition from AHB to occult HBV, suggesting cell-to-cell transmission as the primary driver of occult HBV infection. This conclusion is supported by the observation of clusters of virus-infected cells [2], which may arise from the transfer of nucleocapsids through virological synapses and extracellular vesicles. Goyal et al. found that occult HBV development is not solely dependent on viral suppression but also on inhibiting HBsAg production and export from cccDNA and integrated HBV DNA. In addition, emerging evidence suggests the existence of extra-hepatic sites of HBV replication, such as peripheral blood mononuclear cells, which may significantly influence HBV infection [48–51]. While this aspect has yet to be addressed through modeling, including these sites in this model could lead to a better understanding of HBV dynamics.

3.2 | Acute HBV Models

The BVIM and its variants (Models 1, 2, and 3) exhibit limitations in capturing the dynamics of viral load during AHB infection. These models assume constant rates of infected cell death and virion clearance, which might be suitable for chronic infections (viremia steady state) but fail to reflect the dynamic immune response during primary infection [36, 37]. Neglecting the adaptive nature of the immune response, particularly the nonlinear increase in cellular immunity and humoral clearance, is a major limitation. Consequently, these models faced challenges to appropriately replicate acute, self-limiting disease, emphasizing the need for more realistic immune response modeling in the next generation of models [40]. Since then, models addressing the host immune response, primary acute infection, and long-term outcomes have helped to deepen our understanding of disease progression and the shift from acute to chronic HBV infection.

3.2.1 | Data for Acute HBV Infection

Models capturing acute HBV infection have been severely limited by the lack of clinical biomarker data. Indeed, all acute HBV infection models reviewed in this tutorial relied on data from just seven patients with acute HBV infection [52, 53]. These patients were identified during a single-source outbreak of HBV infection, where 30 patients were infected via autohemotherapy with a single HBV variant. Remarkably, the seven identified patients were monitored before the onset of clinical hepatitis, allowing for direct quantification of virus-specific lymphocytes. This unique scenario provided an opportunity to investigate aspects of viral dynamics, clinical presentation, and host immune responses during the incubation phase of acute HBV infection.

3.2.2 | Different Hepatocyte Populations

Infected hepatocytes may contain viral cccDNA or may integrate viral DNA into the cellular genome. Later models by

Ciupé et al. explored these distinct hepatocellular subsets to better explain the acute infection data (Models 5 and 6, shown in Figure 7) [54, 55].

3.2.2.1 | Two Populations of Infected Cells. Ciupé et al. [54] categorized infected hepatocytes into two groups in their study: group I_1 containing a single copy of cccDNA, and group I_2 containing up to 50 copies, therefore having distinct levels of transcription activity. Model 5 accounted for potential losses in I_1 cells due to non-cytolytic processes leading to cell recovery, and transition to I_2 with the synthesis of new cccDNA. During cell division, I_2 cells could produce I_1 cells, but reversions to uninfected T cells were considered minimal. During proliferation, it is assumed that I_1 gives rise to one infected cell with a single cccDNA copy and another cell with no cccDNA, under the assumption that cccDNA does not replicate during cell division, thereby maintaining a constant population of cells with one cccDNA. Both infected cell types are susceptible to cytolytic elimination by effector cells. However, despite the increased model complexity, incorporating the I_1 and I_2 subsets did not better explain the data than the model with only one population of infected cells with multiple copies of cccDNA. Moreover, while the model described the HBV DNA data well, it revealed challenges in balancing liver integrity and viral load control: The proliferation rate parameter value resulted in an unrealistic loss of hepatocytes, reaching up to 99% at the peak of infection, but increasing that value led to viral rebound. As a result, other mechanisms striking a balance between sustained liver integrity and viral load control had to be considered.

3.2.2.2 | Refractory Cells Population, Model 6. Ciupé et al. [55] further explored the relevance of refractory cells and their role in reinfection in Model 6. Infected cells are depicted as a single class with multiple cccDNA copies. Infected cells can transform into refractory cells dependent on the non-cytolytic action of effector cells and may eventually revert to uninfected cells. The concept of cells becoming refractory to reinfection or resistant to viral replication is crucial for preventing viral resurgence as uninfected cells regenerate. The models fail to capture the data and demonstrate characteristic oscillation in viral load without these refractory cells, attributed to excessive generation of target cells.

3.2.3 | Cellular Adaptive Immune Response

The previously discussed models capture various aspects of the viral dynamics and hepatocyte infection but fail to fully consider immune system dynamics or cytolytic effects. Ciupé et al. [54, 55] addressed this gap by explicitly integrating the immune response into their mathematical model. They illustrated the significant role of cell-mediated immune responses in controlling the virus post-peak in viral load, highlighting their critical roles in both viral clearance and disease progression. Furthermore, modeling results supported the proposal of Guidotti et al. [39] regarding the role of the noncytolytic process in viral clearance. They demonstrated that the initial rapid decline in HBV DNA levels coincided with the peak of the noncytolytic immune response. This suggested that the cytolytic response played a role later in the infection by eliminating infected hepatocytes, while noncytotoxic T-cell effector mechanisms inhibit viral

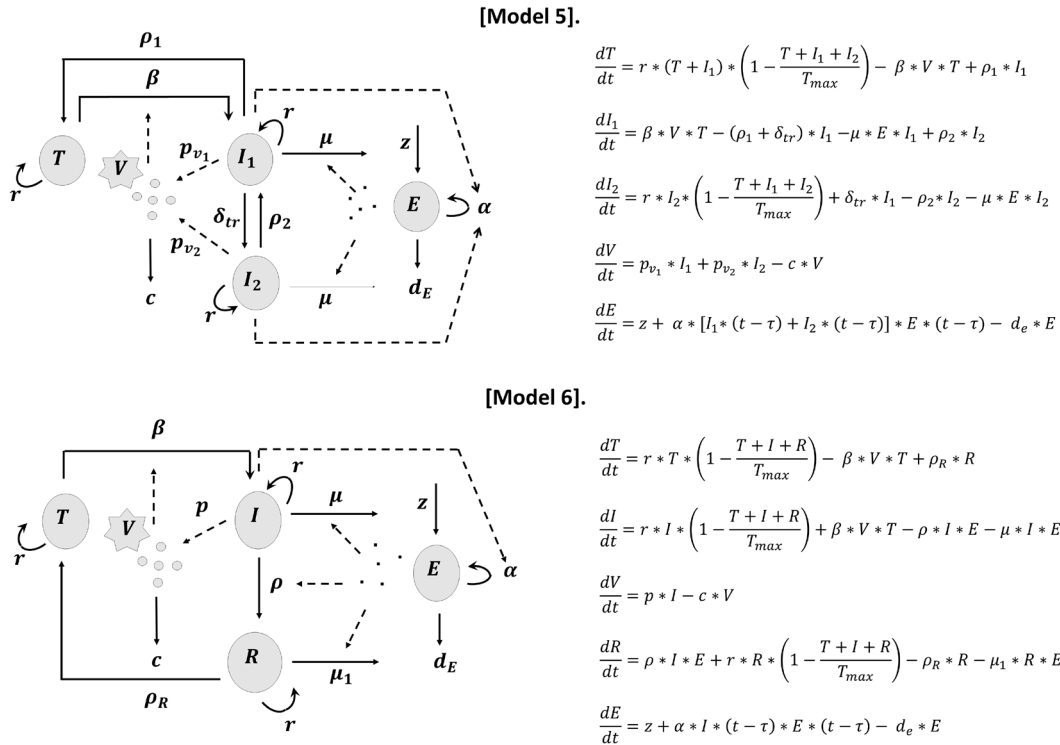


FIGURE 7 | [Model 5]. Acute HBV. Five compartments: T, target uninfected hepatocytes; I_1 , single copy of cccDNA-infected cells; I_2 , 50 copies of cccDNA-infected cells; V, hepatitis B virus; E, immune effector cells (cellular adaptive response). r , uninfected cells proliferation rate; T_{max} , maximum hepatocyte density; β , infection rate; ρ_1 , noncytolytic cure rate of infected cells I_1 ; δ_{tr} , transition rate of I_1 cells to the I_2 class; ρ_2 , noncytolytic cure rate of infected cells I_2 ; μE , cytolytic elimination rate by effector cells (E); p_{v_1} , virions production rate from infected cells I_1 ; p_{v_2} , virions production rate from infected cells I_2 ; c , virions clearance rate; z , source of CD8+ T cells specific to HBV; α , activation and expansion rate of effector cells; τ , time delay in activation and expansion (antigen processing, antigen presentation, interactions between antigen-presenting cells and antigen-specific CD8+ T cells, and the subsequent activation and migration of these cells from lymphoid tissue to the liver); d_E , loss rate of effector cells. [Model 6]. Acute HBV. Five compartments: T, target uninfected hepatocytes; I, infected cells with multiple cccDNA copies; R, refractory cells; V, hepatitis B virus; E, immune effector cells (cellular adaptive response). r , uninfected cells proliferation rate; T_{max} , maximum hepatocyte density; β , infection rate; ρ_R , noncytolytic cure rate of refractory cells R; ρ , noncytolytic cure rate of infected cells I; μE , cytolytic elimination rate of infected cells by effector cells (E); p , virions production rate from infected cells I; c , virions clearance rate; $\mu_1 E$, cytolytic elimination rate of refractory cells by effector cells (E); z , source of CD8+ T cells specific to HBV; α , activation and expansion rate of effector cells; τ , time delay in activation and expansion; d_E , loss rate of effector cell.

replication during early HBV clearance. ALT levels, indicative of hepatocyte damage, exhibited a strong correlation with the cell-mediated immune response, indicating the model effectively captures cytolytic immune response dynamics.

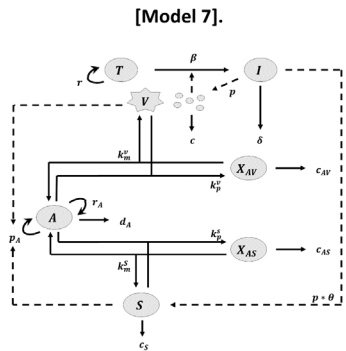
3.2.4 | Humoral Adaptive Immune Response and HBsAg

B-cell-mediated humoral immunity is thought to play a crucial role in controlling viral infection and circulating HBsAg beyond CD8+ effector T cells. Several models, for example, Ciupe et al. [56], delved into the protective mechanisms of the antibody response, with a focus on non-infectious HBV particles like SVPs which are thought to serve as a decoy for the infectious Dane particles [1, 9], allowing HBV to evade the immune system and persist in the host. Their study introduced an antibody model (Model 7, shown in Figure 8) and its variations, which considered uninfected and infected hepatocytes but omitted the recovery of infected cells. This model also accounted for free antibodies generated in response to antigen load, encompassing both viral and

subviral components. The inclusion of a logistic term in the antibody differential equation facilitated the representation of antibodies persisting after viral clearance due to antigen-independent proliferation of memory B cells and long-lived plasma cells. Additionally, the model addressed antigen elimination through the formation of antigen-antibody complexes.

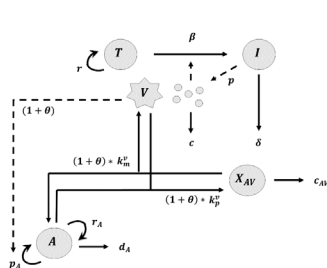
A variation of this model, Model 7a (Figure 8), assumed a quasi-steady state between SVPs and the free virus. The simulations revealed that the predicted quantities of free antibodies necessary for clearance far surpassed typical clinical observations in unvaccinated individuals, suggesting the need for additional mechanisms such as effector CD8+ T cells (Model 7b, shown in Figure 8). These models accurately depicted the transient nature of primary HBV infection, influenced by antibody presence. When anti-HBV antibody levels are high, such as with a vaccine, individuals can achieve clearance if the rate of subviral particle synthesis is slow. Similarly, viral clearance can occur if SVP synthesis is high when anti-HBV antibody production is rapid, antibody affinity is high, or HBV-specific antibodies are elevated at the time of infection, achievable

Panel A.



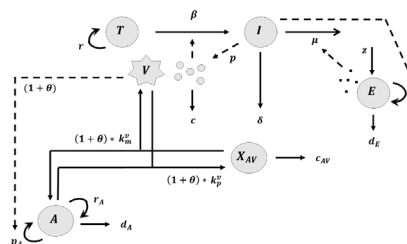
$$\begin{aligned} \frac{dT}{dt} &= r + T * \left(1 - \frac{T+I}{T_{max}}\right) - \beta * V * T \\ \frac{dI}{dt} &= \beta * V * T - \delta * I \\ \frac{dA}{dt} &= p_A * (V+S) + r_A * A * \left(1 - \frac{A}{A_{max}}\right) + k_m^v * X_{AV} + k_m^s * X_{AS} - k_p^v * A * V - k_p^s * A * S - d_A * A \\ \frac{dX_{AV}}{dt} &= k_p^v * A * V - k_m^v * X_{AV} - c_{AV} * X_{AV} \\ \frac{dX_{AS}}{dt} &= k_p^s * A * S - k_m^s * X_{AS} - c_{AS} * X_{AS} \\ \frac{dV}{dt} &= p * I - c * V + k_m^v * X_{AV} - k_p^v * A * V \\ \frac{dS}{dt} &= p * \theta * I - c_s * S + k_m^s * X_{AS} - k_p^s * A * S \end{aligned}$$

[Model 7a].



$$\begin{aligned} \frac{dT}{dt} &= r + T * \left(1 - \frac{T+I}{T_{max}}\right) - \beta * V * T \\ \frac{dI}{dt} &= \beta * V * T - \delta * I \\ \frac{dA}{dt} &= p_A * (1 + \theta) * V + r_A * A * \left(1 - \frac{A}{A_{max}}\right) + (1 + \theta) * k_m^v * X_{AV} - (1 + \theta) * k_p^v * A * V - d_A * A \\ \frac{dX_{AV}}{dt} &= k_p^v * A * V - k_m^v * X_{AV} - c_{AV} * X_{AV} \\ \frac{dV}{dt} &= p * I - c * V + k_m^v * X_{AV} - k_p^v * A * V \end{aligned}$$

[Model 7b].



$$\begin{aligned} \frac{dT}{dt} &= r + T * \left(1 - \frac{T+I}{T_{max}}\right) - \beta * V * T \\ \frac{dI}{dt} &= \beta * V * T - \delta * I - \mu * I + E \\ \frac{dA}{dt} &= p_A * (1 + \theta) * V + r_A * A * \left(1 - \frac{A}{A_{max}}\right) + (1 + \theta) * k_m^v * X_{AV} - (1 + \theta) * k_p^v * A * V - d_A * A \\ \frac{dX_{AV}}{dt} &= k_p^v * A * V - k_m^v * X_{AV} - c_{AV} * X_{AV} \\ \frac{dV}{dt} &= p * I - c * V + k_m^v * X_{AV} - k_p^v * A * V \\ \frac{dE}{dt} &= z + \alpha * I * (t - \tau) * E + (t - \tau) - d_E * E \end{aligned}$$

Panel B.

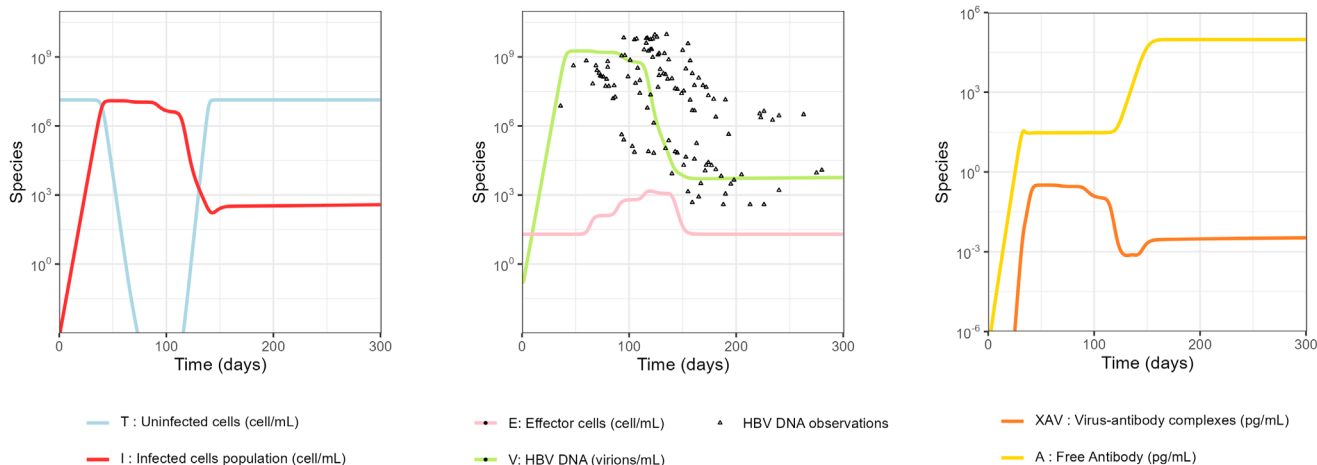


FIGURE 8 | (A) Models' structure and representation: [Model 7]. Acute HBV. Eight compartments: T, Target uninfected hepatocytes; I, infected cells; V, hepatitis B virus; S, subviral particles (SVPs); A, free antibody (humoral adaptive response); X_{AV} and X_{AS} , complexes formed between antibody and the viral and SVPs, respectively. r , uninfected cells proliferation rate; T_{max} , maximum hepatocyte density; β , infection rate; δ , infected cells death rate; p_A , antibody production rate; r_A , antibody maximum proliferation rate; A_{max} , maximum carrying capacity of antibody; d_A , antibody degradation rate; k_p^v and k_p^s , binding rate constants for antibody reacting to viral and SVPs, respectively; k_m^v and k_m^s , disassociation rate constants for antibody reacting to viral and SVPs, respectively; c_{AV} , and c_{AS} , complexes degradation constant rates; p , virions production rate from infected cells I; c , virions clearance rate; $p\theta$, SVPs production rate; c_s , SVPs clearance rate. [Model 7a]. Acute HBV. Five compartments: T, target uninfected hepatocytes; I, infected cells; V, hepatitis B virus; A, free antibody (humoral adaptive response); X_{AV} , complexes formed between antibody and the virions. θ , subvirus-to-virus ratio. [Model 7b]. Acute HBV. Six compartments: T, target uninfected hepatocytes; I, infected cells; V, hepatitis B virus; A, free antibody (humoral adaptive response); X_{AV} , complexes formed between antibody and the virions; E, immune effector cells (cellular adaptive response). μE , cytolytic elimination rate of infected cells by effector cells (E); z , source of CD8+ T cells specific to HBV; α , activation and expansion rate of effector cells; τ , time delay in activation and expansion; d_E , loss rate of effector cell. (B) Species mean profiles simulation of Model 7b: Simulation results of Model 7b over 300 days utilizing mean parameter values and incorporating individual observations for viral load and ALT.

through vaccination. These conditions are crucial for effective clearance. Conversely, if anti-HBV antibody levels are low, a robust cellular immune response involving CD8+ T cells is essential for controlling the initial burst of viral replication.

Subsequently, antibodies become vital for preventing virus rebound and reinfection at later stages. Therefore, both cellular and humoral responses must coordinate to clear AHB infection in these patients.

In summary, this study, along with prior works [54–56], underscores that AHB can be effectively managed through multiple approaches: (1) having high pre-existing antibody levels, (2) relying on a strong initial cellular immune response followed by the development of protective antibodies, and (3) fostering a robust cytopathic and non-cytopathic cellular response that provides lasting protection to hepatocytes against reinfection.

3.2.5 | Infected Hepatocytes Proliferation

The proliferation of infected hepatocytes as well as the resolution of infection through cytolytic or noncytolytic process both play critical roles in governing the dynamics of HBV infection.

For example, successful immune clearance of HBV from the liver appears to occur when cccDNA is lost during hepatocellular mitosis [57]. Addressing this, Ciupe et al. incorporated infected hepatocyte proliferation in an acute infection context and considered spontaneous recovery through cccDNA dilution [54, 55]. Additionally, Goyal et al. explored the role of infected cell proliferation and concomitant loss of cccDNA in aiding the adaptive immune response for AHB infection clearance [58]. Their results suggested that clearance of AHB infection likely depends on cellular proliferation, leading to the generation of two uninfected cells. Their models also considered the addition of cytokine-mediated “cure” in certain scenarios.

Another model addressing the role of cccDNA loss during cell proliferation in AHB was developed by Murray et al. [59] Their results suggested that a cytolytic effect alone is insufficient for clearing the infection. They also demonstrated that, in the absence of refractory cells, partial cccDNA loss combined with cytolytic and noncytolytic effects could clear AHB infection, but at the cost of significant hepatocyte turnover (HT), resulting in substantial liver damage. Therefore, the presence of refractory cells is pivotal if only partial cccDNA clearance occurs during cell proliferation. Conversely, complete cccDNA loss, without refractory cells, leads to AHB clearance with a HT within acceptable limits [57]. This underscores the significance of cccDNA clearance in AHB. Elevated HT levels indicate consequent hepatic injury, which is not characteristic of AHB. Thus, alternative mechanisms must be considered, such as introducing refractory cells to achieve HBV clearance with acceptable HT levels when only partial cccDNA clearance occurs.

3.3 | Other Models of HBV Infection

Several additional models have been proposed in the literature addressing various aspects of HBV infection biology beyond the models already reviewed.

3.3.1 | ALT Model

ALT represents a clinically meaningful biomarker of liver inflammation after active viral replication. This biomarker has

been included in models by Su et al. [60], Ciupe et al. [61], and others. The model developed by Su et al. [60] robustly captures clinical data on ALT and HBV DNA. Similarly, Ciupe et al. [61] developed a comprehensive mathematical framework of HBV infection integrating ALT, although their primary focus lay on investigating the impact of inoculum dose on infection outcomes. Their model captures HBV DNA and ALT data from HBV-naive adult chimpanzees and concluded that inoculum dose influences both the timing and quality of CD8 T-cell expansion, particularly in terms of noncytotoxic function.

3.3.2 | Intracellular Model

While simpler models focus on the interplay between the virus, cells, and possibly antibodies, more sophisticated models aim to also capture the intracellular hepatocyte dynamics to provide a better understanding of clearance mechanisms, enabling the rational design of treatment strategies. For instance, Murray et al. [62] used data from acutely HBV-infected chimpanzees to study the export of the virus from infected hepatocytes. They revealed that the half-life of HBV in the blood is considerably shorter than earlier estimates by incorporating preformed mature DNA-containing HBV capsids into the model. Their findings suggest a maximum half-life of only 4.4 h, which significantly differs from the previous estimate of 1 day [31–33, 38]. This study highlights that the slow viral clearance is primarily due to the rate of viral export from infected hepatocytes rather than the long half-life of free virus in the bloodstream. Their findings indicate that the decay of HBV DNA in the bloodstream during immune clearance correlates more closely with changes in intracellular HBV DNA levels than with extracellular processes.

3.3.3 | Innate Immunity Model

A study conducted by Fatehi et al. [63] presented a comprehensive mathematical model that more broadly encompasses the dynamics of the immune response to HBV. This model includes refractory cells, the response of effector cells, and the production of HBsAg antibodies and cytokines. While they also included aspects of the innate immune response, its role in resolving AHB infection has been a topic of debate. Indeed, experimental evidence suggested that during AHB, HBV elicits minimal or no innate immune responses [3].

3.3.4 | Multiscale Model

The models reviewed so far all consider the interaction between virus and various cellular and molecular components of the immune system during HBV infection. However, most do not address the influence of spatial distribution throughout infection. Several authors have addressed this in their modeling efforts. For example, Cangelosi et al. [64] developed a comprehensive multiscale model and concluded that HBV exploits the spatial characteristics of the liver environment, with liver spatial patterns contributing to the persistence of HBV infections. Similarly, Kitagawa et al. [65] built a multiscale model quantifying cccDNA in the liver along with intracellular and intercellular HBV infection processes. They applied this model to in vitro

and vivo experimental data as well as specific surrogate viral markers in serum, such as HBV DNA, HBsAg, HBeAg, and HBcrAg to predict the dynamics of intrahepatic cccDNA. By incorporating a relevant clinical endpoint such as intrahepatic cccDNA dynamics, this approach may provide valuable insight for further therapeutic development in CHB.

3.4 | Numerical Simulations Using R and RShiny

We have reviewed several models for hepatitis B infection and viral dynamics of varying complexity in this tutorial. While we attempted to describe in sufficient detail the nature of each model and the accompanying mathematical formulism, we find that the best way to fully understand the behavior of these models is through interactive visualization. We have developed an interactive RShiny app that implements several models, including Models 5–7b, to aid readers in understanding the dynamics of HBV infection. The app can be used to visualize either the population mean (Code S1) or individual profiles (Code S2). Using Code S1, we simulated Model 7b over 300 days with the provided mean parameter values and initial conditions (Tables S2 and S3), shown in Figure 8B. The simulation demonstrates that cytotoxic effects lead to the initial viral control (middle plot), while antibodies play a crucial role in preventing re-infection (right plot). These antibodies act similarly to the immune refractory state of target cells described in Model 6, with their effects closely aligned with antibody levels and timing. This analysis also integrates individual observations for viral load (HBV DNA), showcasing the model's capability of accurately representing these data points. Readers can adjust parameter values, initial conditions, and simulation durations to observe their impact on viral dynamics. For instance, by setting the r parameter (proliferation rate) from 0.01 to 1 in Model 5, as done in Models 6–7b, oscillations in the HBV DNA profile emerge, and HBV DNA clearance is no longer observed. These simulations illustrate how the choice of model structure and parameter values can significantly influence predicted behaviors and outcomes. We encourage readers to explore these tools to gain a deeper understanding of the relationship between parameters and the clinical outcomes predicted by different model structures.

4 | Conclusion

This tutorial aimed to highlight the high degree of complexity of the various pathophysiological mechanisms contributing to acute and chronic HBV infection. Accordingly, mathematical models examining the contributions of these mechanisms to the overall disease progression at various stages of the disease are of great utility. We explored the relationship between assumed mathematical model structure and predicted dynamics for both acute and chronic HBV infection. Understanding the differences between these clinical settings requires a detailed study of existing knowledge derived from diverse experimental datasets. Moreover, we emphasized how the generation of new experimental data can necessitate new modeling assumptions and lead to novel model-based insights.

As a pharmacometrician, it is important to determine model complexity in light of the question at hand, while simplifying or even omitting unessential aspects of disease biology. We showed

how the data available and the biological questions of interest helped determine the modeling choices made by the study authors through the examples provided. Importantly, although the more recent models presented might reflect fresh perspectives or new assumptions regarding HBV infection, the scientific community must continue to acquire additional data that can confirm the predictions and assumptions made by these models. This iterative process of learning, confirming, and applying is indispensable for advancing our understanding of the virus and the patient and, ultimately, for developing more effective strategies for its prevention and treatment.

Finally, this tutorial focused on reviewing our evolving understanding of HBV biology and the models developed to explain clinical observations. In a powerful extension, disease progression models coupled with pharmacokinetic–pharmacodynamic modeling allows for a quantitative evaluation of the effects of drug treatments on disease progression. This approach has been demonstrated in various studies, showcasing its potential to provide a deeper understanding of the intricate relationship between modeling and drug therapy in managing viral infections.

Acknowledgments

The authors would like to thank Dr. Valvanera Vozmediano Esteban and Dr. Ana Ruiz for their support in the development of this tutorial.

The Shiny apps code can be found in Github by following the link: <https://github.com/cboivinchampeaux/Acute-HBV-models>, or in the PDF document Code S1.pdf and Code S2.pdf to see the mean profiles and individual profiles, respectively, for the different models.

Conflicts of Interest

The authors declare no conflicts of interest.

References

1. C. Herrscher, P. Roingard, and E. Blanchard, "Hepatitis B Virus Entry Into Cells," *Cells* 9, no. 6 (2020): 1486, <https://doi.org/10.3390/cells9061486>.
2. P. Karayiannis, "Hepatitis B Virus: Virology, Molecular Biology, Life Cycle and Intrahepatic Spread," *Hepatology International* 11, no. 6 (2017): 500–508, <https://doi.org/10.1007/s12072-017-9829-7>.
3. M. Iannacone and L. G. Guidotti, "Immunobiology and Pathogenesis of Hepatitis B Virus Infection," *Nature Reviews. Immunology* 22, no. 1 (2022): 19–32, <https://doi.org/10.1038/s41577-021-00549-4>.
4. L. Wei and A. Ploss, "Mechanism of Hepatitis B Virus cccDNA Formation," *Viruses* 13, no. 8 (2021): 1463, <https://doi.org/10.3390/v13081463>.
5. W. Gao and J. Hu, "Formation of Hepatitis B Virus Covalently Closed Circular DNA: Removal of Genome-Linked Protein," *Journal of Virology* 81, no. 12 (2007): 6164–6174, <https://doi.org/10.1128/JVI.02721-06>.
6. M. A. Mendenhall, X. Hong, and J. Hu, "Hepatitis B Virus Capsid: The Core in Productive Entry and Covalently Closed Circular DNA Formation," *Viruses* 15, no. 3 (2023): 642, <https://doi.org/10.3390/v15030642>.
7. T. Tu, M. Budzinska, N. Shackel, and S. Urban, "HBV DNA Integration: Molecular Mechanisms and Clinical Implications," *Viruses* 9, no. 4 (2017): 75, <https://doi.org/10.3390/v9040075>.
8. T. Watanabe, E. M. Sorensen, A. Naito, M. Schott, S. Kim, and P. Ahlquist, "Involvement of Host Cellular Multivesicular Body Functions

- in Hepatitis B Virus Budding," *Proceedings of the National Academy of Sciences* 104, no. 24 (2007): 10205–10210, <https://doi.org/10.1073/pnas.0704000104>.
9. M. Bruns, S. Miska, S. Chassot, and H. Will, "Enhancement of Hepatitis B Virus Infection by Noninfectious Subviral Particles," *Journal of Virology* 72, no. 2 (1998): 1462–1468, <https://doi.org/10.1128/JVI.72.2.1462-1468.1998>.
10. E. Sivasudhan, N. Blake, Z. Lu, J. Meng, and R. Rong, "Hepatitis B Viral Protein HBx and the Molecular Mechanisms Modulating the Hallmarks of Hepatocellular Carcinoma: A Comprehensive Review," *Cells* 11, no. 4 (2022): 741, <https://doi.org/10.3390/cells11040741>.
11. W. J. Jeng, G. V. Papatheodoridis, and A. S. F. Lok, "Hepatitis B," *Lancet* 401, no. 10381 (2023): 1039–1052, [https://doi.org/10.1016/S0140-6736\(22\)01468-4](https://doi.org/10.1016/S0140-6736(22)01468-4).
12. C. Seeger and W. S. Mason, "Molecular Biology of Hepatitis B Virus Infection," *Virology* 479–480 (2015): 672–686, <https://doi.org/10.1016/j.virol.2015.02.031>.
13. Y. H. Shi and C. H. Shi, "Molecular Characteristics and Stages of Chronic Hepatitis B Virus Infection," *World Journal of Gastroenterology* 15, no. 25 (2009): 3099–3105, <https://doi.org/10.3748/wjg.15.3099>.
14. L. G. Guidotti, T. Ishikawa, M. V. Hobbs, B. Matzke, R. Schreiber, and F. V. Chisari, "Intracellular Inactivation of the Hepatitis B Virus by Cytotoxic T Lymphocytes," *Immunity* 4, no. 1 (1996): 25–36, [https://doi.org/10.1016/S1074-7613\(00\)80295-2](https://doi.org/10.1016/S1074-7613(00)80295-2).
15. F. V. Chisari, M. Isogawa, and S. F. Wieland, "Pathogenesis of Hepatitis B Virus Infection," *Pathologie et Biologie* 58, no. 4 (2010): 258–266, <https://doi.org/10.1016/j.patbio.2009.11.001>.
16. H. J. Yim and A. S. F. Lok, "Natural History of Chronic Hepatitis B Virus Infection: What We Knew in 1981 and What We Know in 2005," *Hepatology* 43, no. S1 (2006): S173–S181, <https://doi.org/10.1002/hep.20956>.
17. C. S. Coffin, K. Zhou, and N. A. Terrault, "New and Old Biomarkers for Diagnosis and Management of Chronic Hepatitis B Virus Infection," *Gastroenterology* 156, no. 2 (2019): 355–368, <https://doi.org/10.1053/j.gastro.2018.11.037>.
18. A. Kramvis, K. M. Chang, M. Dandri, et al., "A Roadmap for Serum Biomarkers for Hepatitis B Virus: Current Status and Future Outlook," *Nature Reviews. Gastroenterology & Hepatology* 19, no. 11 (2022): 727–745, <https://doi.org/10.1038/s41575-022-00649-z>.
19. A. P. Bénéchet, G. De Simone, P. Di Lucia, et al., "Dynamics and Genomic Landscape of CD8+ T Cells Undergoing Hepatic Priming," *Nature* 574, no. 7777 (2019): 200–205, <https://doi.org/10.1038/s41586-019-1620-6>.
20. M. Chen, M. Sällberg, J. Hughes, et al., "Immune Tolerance Split Between Hepatitis B Virus Precore and Core Proteins," *Journal of Virology* 79, no. 5 (2005): 3016–3027, <https://doi.org/10.1128/JVI.79.5.3016-3027.2005>.
21. N. Alatrakchi and M. Koziel, "Regulatory T Cells and Viral Liver Disease," *Journal of Viral Hepatitis* 16, no. 4 (2009): 223–229, <https://doi.org/10.1111/j.1365-2893.2009.01081.x>.
22. X. Li, Y. Chen, Z. Ma, B. Ye, W. Wu, and L. Li, "Effect of Regulatory T Cells and Adherent Cells on the Expansion of HBcAg-Specific CD8+ T Cells in Patients With Chronic Hepatitis B Virus Infection," *Cellular Immunology* 264, no. 1 (2010): 42–46, <https://doi.org/10.1016/j.cellimm.2010.04.009>.
23. L. Zhao, D. K. Qiu, and X. Ma, "Th17 Cells: The Emerging Reciprocal Partner of Regulatory T Cells in the Liver," *Journal of Digestive Diseases* 11, no. 3 (2010): 126–133, <https://doi.org/10.1111/j.1751-2980.2010.00428.x>.
24. Y. C. Chen, C. M. Chu, and Y. F. Liaw, "Age-Specific Prognosis Following Spontaneous Hepatitis B e Antigen Seroconversion in Chronic Hepatitis B," *Hepatology* 51, no. 2 (2010): 435–444, <https://doi.org/10.1002/hep.23348>.
25. S. K. Sharma, N. Saini, and Y. Chwla, "Hepatitis B Virus: Inactive Carriers," *Virology Journal* 2 (2005): 82, <https://doi.org/10.1186/1743-422X-2-82>.
26. C. L. Lin and J. H. Kao, "New Perspectives of Biomarkers for the Management of Chronic Hepatitis B," *Clinical and Molecular Hepatology* 22, no. 4 (2016): 423–431, <https://doi.org/10.3350/cmh.2016.0069>.
27. European Association for the Study of the Liver, "EASL Clinical Practice Guidelines: Management of Chronic Hepatitis B Virus Infection," *Journal of Hepatology* 57, no. 1 (2012): 167–185, <https://doi.org/10.1016/j.jhep.2012.02.010>.
28. T. Tu, F. van Bömmel, and T. Berg, "Surrogate Markers for Hepatitis B Virus Covalently Closed Circular DNA," *Seminars in Liver Disease* 42, no. 03 (2022): 327–340, <https://doi.org/10.1055/a-1830-2741>.
29. T. C. F. Yip, G. L. H. Wong, V. W. S. Wong, et al., "Durability of Hepatitis B Surface Antigen Seroclearance in Untreated and Nucleos(t)ide Analogue-Treated Patients," *Journal of Hepatology* 68, no. 1 (2018): 63–72, <https://doi.org/10.1016/j.jhep.2017.09.018>.
30. V. R. Knight-Schrijver, V. Chelliah, L. Cucurull-Sanchez, and N. Le Novère, "The Promises of Quantitative Systems Pharmacology Modelling for Drug Development," *Computational and Structural Biotechnology Journal* 14 (2016): 363–370, <https://doi.org/10.1016/j.csbj.2016.09.002>.
31. M. A. Nowak, S. Bonhoeffer, A. M. Hill, R. Boehme, H. C. Thomas, and H. McDade, "Viral Dynamics in Hepatitis B Virus Infection," *Proceedings of the National Academy of Sciences* 93, no. 9 (1996): 4398–4402, <https://doi.org/10.1073/pnas.93.9.4398>.
32. M. Tsiang, J. F. Rooney, J. J. Toole, and C. S. Gibbs, "Biphasic Clearance Kinetics of Hepatitis B Virus From Patients During Adefovir Dipivoxil Therapy," *Hepatology* 29, no. 6 (1999): 1863–1869, <https://doi.org/10.1002/hep.510290626>.
33. G. K. Lau, M. Tsiang, J. Hou, et al., "Combination Therapy With Lamivudine and Famciclovir for Chronic Hepatitis B-Infected Chinese Patients: A Viral Dynamics Study," *Hepatology* 32, no. 2 (2000): 394–399, <https://doi.org/10.1053/jhep.2000.9143>.
34. L. Min, Y. Su, and Y. Kuang, "Mathematical Analysis of a Basic Virus Infection Model With Application to HBV Infection," *Rocky Mountain Journal of Mathematics* 38, no. 5 (2008): 1573–1586, <https://doi.org/10.1216/RMJ-2008-38-5-1573>.
35. S. A. Gourley, Y. Kuang, and J. D. Nagy, "Dynamics of a Delay Differential Equation Model of Hepatitis B Virus Infection," *Journal of Biological Dynamics* 2, no. 2 (2008): 140–153, <https://doi.org/10.1080/17513750701769873>.
36. R. M. Ribeiro, A. Lo, and A. S. Perelson, "Dynamics of Hepatitis B Virus Infection," *Microbes and Infection* 4, no. 8 (2002): 829–835, [https://doi.org/10.1016/S1286-4579\(02\)01603-9](https://doi.org/10.1016/S1286-4579(02)01603-9).
37. A. S. Perelson and R. M. Ribeiro, "Hepatitis B Virus Kinetics and Mathematical Modeling," *Seminars in Liver Disease* 24 (2004): 11–16, <https://doi.org/10.1055/s-2004-828673>.
38. S. Lewin, "Analysis of Hepatitis B Viral Load Decline Under Potent Therapy: Complex Decay Profiles Observed," *Hepatology* 34, no. 5 (2001): 1012–1020, <https://doi.org/10.1053/jhep.2001.28509>.
39. L. G. Guidotti, R. Rochford, J. Chung, M. Shapiro, R. Purcell, and F. V. Chisari, "Viral Clearance Without Destruction of Infected Cells During Acute HBV Infection," *Science* 284, no. 5415 (1999): 825–829, <https://doi.org/10.1126/science.284.5415.825>.
40. S. Eikenberry, S. Hews, J. D. Nagy, and Y. Kuang, "The Dynamics of a Delay Model of Hepatitis B Virus Infection With Logistic Hepatocyte Growth," *Mathematical Biosciences and Engineering* 6, no. 2 (2009): 283–299, <https://doi.org/10.3934/mbe.2009.6.283>.
41. S. Hews, S. Eikenberry, J. D. Nagy, and Y. Kuang, "Rich Dynamics of a Hepatitis B Viral Infection Model With Logistic Hepatocyte Growth," *Journal of Mathematical Biology* 60, no. 4 (2010): 573–590, <https://doi.org/10.1007/s00285-009-0278-3>.

42. G. K. Michalopoulos, "Liver regeneration," *Journal of Cellular Physiology* 213, no. 2 (2007): 286–300, <https://doi.org/10.1002/jcp.21172>.
43. J. Rozga, "Hepatocyte Proliferation in Health and in Liver Failure," *Medical Science Monitor* 7, no. Suppl 1 (2002): 78–90.
44. S. M. Ciupe and S. Hews, "Mathematical Models of E-Antigen Mediated Immune Tolerance and Activation Following Prenatal HBV Infection," *PLoS One* 7, no. 7 (2012): e39591, <https://doi.org/10.1371/journal.pone.0039591>.
45. S. Kadelka and S. M. Ciupe, "Department of Mathematics, Virginia Polytechnic Institute and State University, Blacksburg, VA 24061, USA. Mathematical Investigation of HBeAg Seroclearance," *Mathematical Biosciences and Engineering* 16, no. 6 (2019): 7616–7658, <https://doi.org/10.3934/mbe.2019382>.
46. H. L. Y. Chan, M. Hussain, and A. S. F. Lok, "Different Hepatitis B Virus Genotypes Are Associated With Different Mutations in the Core Promoter and Precore Regions During Hepatitis B e Antigen Seroconversion," *Hepatology* 29, no. 3 (1999): 976–984, <https://doi.org/10.1002/hep.510290352>.
47. A. Goyal and R. Chauhan, "The Dynamics of Integration, Viral Suppression and Cell-Cell Transmission in the Development of Occult Hepatitis B Virus Infection," *Journal of Theoretical Biology* 455 (2018): 269–280, <https://doi.org/10.1016/j.jtbi.2018.06.020>.
48. S. Datta, "Compartmentalization of Hepatitis B Virus: Looking Beyond the Liver," *World Journal of Hepatology* 7, no. 20 (2015): 2241, <https://doi.org/10.4254/wjh.v7.i20.2241>.
49. S. Stoll-Becker, R. Repp, D. Glebe, et al., "Transcription of Hepatitis B Virus in Peripheral Blood Mononuclear Cells From Persistently Infected Patients," *Journal of Virology* 71, no. 7 (1997): 5399–5407, <https://doi.org/10.1128/jvi.71.7.5399-5407.1997>.
50. S. Gao, Z. P. Duan, Y. Chen, et al., "Compartmental HBV Evolution and Replication in Liver and Extrahepatic Sites After Nucleos/Tide Analogue Therapy in Chronic Hepatitis B Carriers," *Journal of Clinical Virology* 94 (2017): 8–14, <https://doi.org/10.1016/j.jcv.2017.06.009>.
51. Y. Murakami, M. Minami, Y. Daimon, and T. Okanou, "Hepatitis B Virus DNA in Liver, Serum, and Peripheral Blood Mononuclear Cells After the Clearance of Serum Hepatitis B Virus Surface Antigen," *Journal of Medical Virology* 72, no. 2 (2004): 203–214, <https://doi.org/10.1002/jmv.10547>.
52. G. Webster, "Incubation Phase of Acute Hepatitis B in Man: Dynamic of Cellular Immune Mechanisms," *Hepatology* 32, no. 5 (2000): 1117–1124, <https://doi.org/10.1053/jhep.2000.19324>.
53. S. A. Whalley, J. M. Murray, D. Brown, et al., "Kinetics of Acute Hepatitis B Virus Infection in Humans," *Journal of Experimental Medicine* 193, no. 7 (2001): 847–854, <https://doi.org/10.1084/jem.193.7.847>.
54. S. M. Ciupe, R. M. Ribeiro, P. W. Nelson, and A. S. Perelson, "Modeling the Mechanisms of Acute Hepatitis B Virus Infection," *Journal of Theoretical Biology* 247, no. 1 (2007): 23–35, <https://doi.org/10.1016/j.jtbi.2007.02.017>.
55. S. M. Ciupe, R. M. Ribeiro, P. W. Nelson, G. Dusheiko, and A. S. Perelson, "The Role of Cells Refractory to Productive Infection in Acute Hepatitis B Viral Dynamics," *Proceedings of the National Academy of Sciences* 104, no. 12 (2007): 5050–5055, <https://doi.org/10.1073/pnas.0603626104>.
56. S. M. Ciupe, R. M. Ribeiro, and A. S. Perelson, "Antibody Responses During Hepatitis B Viral Infection," *PLoS Computational Biology* 10, no. 7 (2014): e1003730, <https://doi.org/10.1371/journal.pcbi.1003730>.
57. J. Summers, A. R. Jilbert, W. Yang, et al., "Hepatocyte Turnover During Resolution of a Transient Hepadnaviral Infection," *Proceedings of the National Academy of Sciences* 100, no. 20 (2003): 11652–11659, <https://doi.org/10.1073/pnas.1635109100>.
58. A. Goyal, R. Ribeiro, and A. Perelson, "The Role of Infected Cell Proliferation in the Clearance of Acute HBV Infection in Humans," *Viruses* 9, no. 11 (2017): 350, <https://doi.org/10.3390/v9110350>.
59. J. M. Murray and A. Goyal, "In Silico Single Cell Dynamics of Hepatitis B Virus Infection and Clearance," *Journal of Theoretical Biology* 366 (2015): 91–102, <https://doi.org/10.1016/j.jtbi.2014.11.020>.
60. Y. Su, Y. Wen, and L. Min, "Analysis of a HBV Infection Model With ALT," in *2012 IEEE 6th International Conference on Systems Biology (ISB)* (Xi'an, China: IEEE, 2012), 97–100, <https://doi.org/10.1109/ISB.2012.6314119>.
61. S. M. Ciupe, N. K. Vaidya, and J. E. Forde, "Early Events in Hepatitis B Infection: The Role of Inoculum Dose," *Proceedings of the Royal Society B: Biological Sciences* 2021, no. 288 (1944): 20202715, <https://doi.org/10.1098/rspb.2020.2715>.
62. J. M. Murray, R. H. Purcell, and S. F. Wieland, "The Half-Life of Hepatitis B Virions," *Hepatology* 44, no. 5 (2006): 1117–1121, <https://doi.org/10.1002/hep.21364>.
63. F. Fatehi Chenar, Y. N. Kyrychko, and K. B. Blyuss, "Mathematical Model of Immune Response to Hepatitis B," *Journal of Theoretical Biology* 447 (2018): 98–110, <https://doi.org/10.1016/j.jtbi.2018.03.025>.
64. Q. Cangelosi, S. A. Means, and H. Ho, "A Multi-Scale Spatial Model of Hepatitis-B Viral Dynamics," *PLoS One* 12, no. 12 (2017): e0188209, <https://doi.org/10.1371/journal.pone.0188209>.
65. K. Kitagawa, K. S. Kim, M. Iwamoto, et al., "Multiscale Modeling of HBV Infection Integrating Intra- and Intercellular Viral Propagation to Analyze Extracellular Viral Markers," *PLoS Computational Biology* 20, no. 3 (2024): e1011238, <https://doi.org/10.1371/journal.pcbi.1011238>.

Supporting Information

Additional supporting information can be found online in the Supporting Information section.